EFFECTIVE STRESS FINITE ELEMENT ANALYSIS OF PILE-SOIL INTERACTION PROBLEMS

Dr. Yousif J.Al-Shakarchi
University of Baghdad

Dr. Mohammed Yousif Fattah
University of Technology

Aram M. Raheem
University of Baghdad.

ABSTRACT

The effective stress method is developed to predict the axial capacity of piles in clay. This method is based on the principle that, at failure, the available shear resistance at the pile soil interface is related to the mean normal effective stress at the pile face and the effective stress friction angle for the soil sliding on the pile material.

In this paper, the coupled non-linear finite element method is used to analyze some pile-soil interaction problems. This computer program (CRISP) is used for this task. Eight- node isoparametric elements were used for displacements while four- node elements are used for pore pressure. Interface elements are used to simulate the interaction between the pile and the soil. The soil is assumed to follow different models, linear elastic and modified Cam-clay model. A comparison is made between the measured and predicted settlements and excess pore water pressures and good convergence was obtained in which the proposed technique used in this paper, in which the measured excess pore water pressures are considered as initial pore pressures in the computer program (CRISP). No load was applied on the pile. The dissipation of excess pore water was studied through carrying out consolidation analysis.

KEY WORDS

Finite Elements, Pile, Effective Stress.

الخلاصة

إن مبدأ الإجهاد الفعال قد اعتمد لتخمين الاستيعاب المحوري للركائز في الطين.وتعتمد هذه الطريقة على مبدأ، انه عند الفشل، ان مقاومة القص المتوفرة عند منطقة التماس بين الركيزة و التربة تعود إلى معدل الإجهاد العمودي الفعال عند وجه الركيزة و إلى زاوية الاحتكاك الداخلي للإجهاد الفعال للتربة المتزحلقة على مادة الركيزة.

في هذا البحث استعملت طريقة التحليل المزدوج بطريقة العناصر المحددة لتحليل بعض مسائل التداخل بين الركيزة والتربة. واستعمل برنامج الحاسبة المسمى (CRISP) لهذا الغرض وقد مثلت المسالة باستخدام عناصر رباعية ثمانية العقد للازاحات وعناصر رباعية العقد لتمثيل ضغط ماء المسام واستخدمت العناصر الانزلاقية لتمثيل التداخل بين الركيزة والتربة. وقد افترض ان التربة تتبع سلوك نماذج مختلفة منها المرن الخطي ونموذج طين كام المعدل.

وقد اجريت مقارنة بين الهبوطات وضغط ماء المسام الاضافي المقاسة والمخمنة بطريقة العناصر المحددة ووجد تقارب جيد بين النتائج.

وقد تم التوصل الى نتائج منها ان التقنية المقترحة والمستعملة في هذا البحث والتي من خلالها مثلت ضغوط ماء المسام المقاسة بكونها ضغوط الماء الابتدائية في برنامج الحاسبة (CRISP) و لم يتم تسليط حمل على الركيزة في هـــذه الحالـــة. ودرس تصريف ضغط ماء المسام الاضافي من خلال اجراء تحليل الانضمام.

INTRODUCTION

The initial development of a general effective stress method for the predication of the axial capacity of driven piles in clay is described by Esrig et al. (1979). This method is based on the principle that, at failure, the available shear resistance at the pile soil interface is related to the mean normal effective stress at the pile face and the effective stress friction angle for the soil sliding on the pile material.

Grande and Nordal (1979) presented a procedure for predication of the pile soil interface stresses by means of effective stress parameters derived from tests performed in oedometer and triaxial tests. They derived several formulas from effective stress soil parameters, which are:

1) The ultimate lateral and axial pile head loads.
2) the soil reaction coefficients:
   $ky = dp/dv$ and $kz = dt/dw$

   Relating the lateral and axial displacements v and w of a pile element to the corresponding soil reactions p and t.
3) simplified dimensionless p-v and t-w curves from which soil reaction curves may be constructed.

Randolph and Wroth (1981) used effective stress analysis to produce a more rational design method for shaft capacity. They discovered that for normally and lightly over-consolidated clay, the experimental data have been shown to be in broad agreement with the theoretically deduced strengths where at higher values of overconsolidation ratio, there will be overestimate in strength.

Numerical analysis

The advancement of modern computers made possible development of sophisticated numerical solution techniques for solving boundary value problems in geotechnical engineering (Al-Chalabi, 1990).

There are different numerical methods such as the finite element method, boundary integral equation method, finite difference method, etc. The finite element method was the important numerical method between others, and will be used in this paper.

Finite Element Program

The computer program CRISP (critical state program) was developed at Cambridge University, Engineering Department, Soil Mechanics Group, in 1975. Later and after making necessary modifications on (CRISP), it was published in 1987, (Britto and Gunn, 1987).

CRISP uses the finite element technique and allows predictions to be made of ground deformation using critical state theories. The program CRISP is used in this work to analyze pile-soil interaction problems after making necessary developments.

Solution techniques

Non-linear response arises from either geometric non-linearity or material non-linearity. Geometric non-linearity arises when large deformations of the structure mean that the equilibrium equations (based on the undeformed structure geometry) are no longer

sufficiently accurate. Material non-linearity arises when the stress-strain relation for the material is non-linear (e.g. the Cam-clay model relations).

There are a number of techniques for analyzing non-linear problems using the finite elements. CRISP uses the incremental or tangent stiffness approach: the user divides the total load acting into a number of small increments and the program applies each of these incremental loads in turn. During each increment, the stiffness properties appropriate for the current stress levels are used in the calculations. If only a few increments are used, this method produces a solution that tends to drift away from the true or exact solution. This means a stiffer response result for a strain-hardening model and the displacements are always under-predicated.

Problem No.1

Desai (1974) used the (FEM) to analyze field pile load tests conducted on pipe piles at the lock and Dam on the Arkansas river in USA. The results of single test performed on one of the piles (pile 3 in the reference) are analyzed here.

The diameter and penetration depth of pile (3) was (0.508) m, (16.15) m respectively. The total load applied on pile (3) was (280) tons through (13) increments, and the finite element mesh for the axisymmetric problem can be seen in Figure (1). Both sides are impermeable for water dissipation. Eight-node isoparametric elements were used for displacements while four-node elements were used for pore pressure.

Material properties

a) **Pile material (steel):** the (stress-strain) behavior of steel was assumed linear elastic. The equivalent elastic modulus (**$E_{eq.}=196*10^5$ kN/m^2**), Poission ratio (**$\upsilon=0.2$**), (the given values are equivalent for pipe steel pile).

b) **Soil (sand):** the (stress-strain) behavior of sand was assumed to be linear isotropic elastic. Table (1) presents the sand properties used in the analysis.

Table (1) Sand properties for problem No.1 (after Desai, 1974).

Property	Modulus of Elasticity E_S (kN/m^2)	Poisson's ratio (υ)	Angle of friction $(\emptyset^\circ)$	Unit weight γ (kN/m^3)	Coefficient of lateral earth pressure K_o
Value	33113.7	0.3	32°	21.2	1.17

c) **Interface material:** the material at the interface and the soil were assumed to have the same properties except that the other properties of the interface were calculated as follows the following procedure of:

Kn: Normal stiffness.

$$Kn = \frac{E(1-\upsilon)}{(1+\upsilon)(1-2\upsilon)}$$

Ks: Shear stiffness.

$$Ks = \frac{E}{2(1+\upsilon)}$$

Kres: Residual shear stiffness.

$$Kres = \left(\frac{1}{100} \text{ to } \frac{1}{1000}\right) Ks$$

t: thickness of element.

$$t = \left(\frac{L}{10} \text{ to } \frac{L}{100} \right)$$

L: length of element.

Through table (2), the interface material properties can be seen.

Table (2) Interface material properties.

Type of soil	c(kPa)	ϕ	*Kn (kPa)*	*Ks (kPa)*	*Kres (kPa)*	*t (m)*
sand	0	32	44547.9	12714	25.457	0.0299

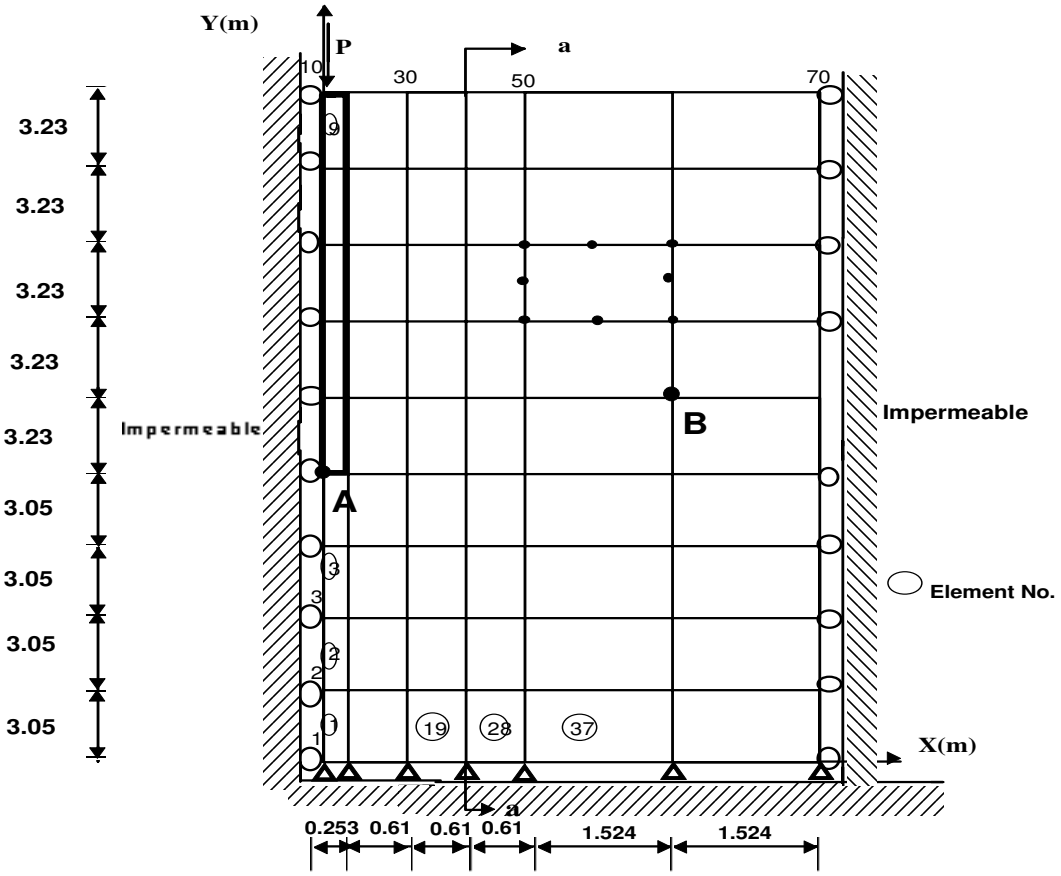

Fig. (1) The finite element mesh for problem No.1.

Due to symmetry in geometry and loading, only one half of the geometry is modelled. Eight-noded quadrilateral elements are used for both the pile and soil materials. The right and left boundaries are restrained horizontally and are free to move vertically. The load was applied in increments to simulate the actual loading. Another mesh was made for pore pressure consisted of eight-node elements for the soil material only.

Results

Fig (2) presents the load-settlement relationship. Figure (3) shows the surface settlement of the pile and adjacent soil predicated at nodes (10, 20, 30, 40, 50, 60 and 70) as shown in Figure (1). Figure (4) shows the changes in vertical effective stress along section (a-a) in the same mesh.

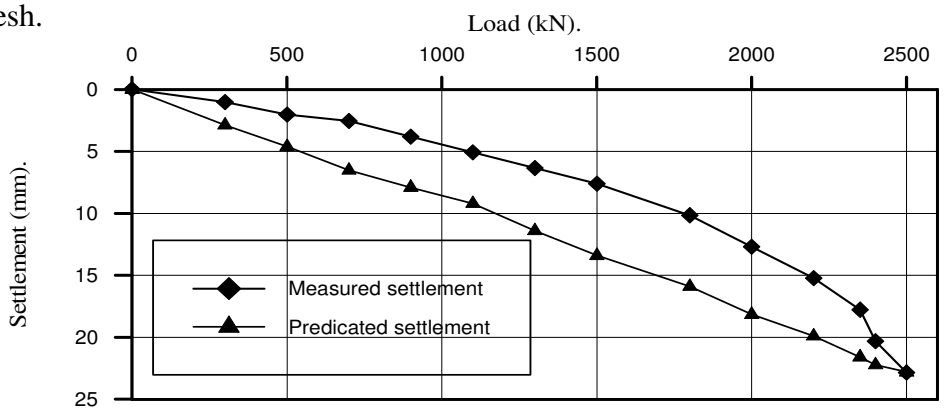

Fig. (2) The load-settlement relationship for the pile of problem No.1.

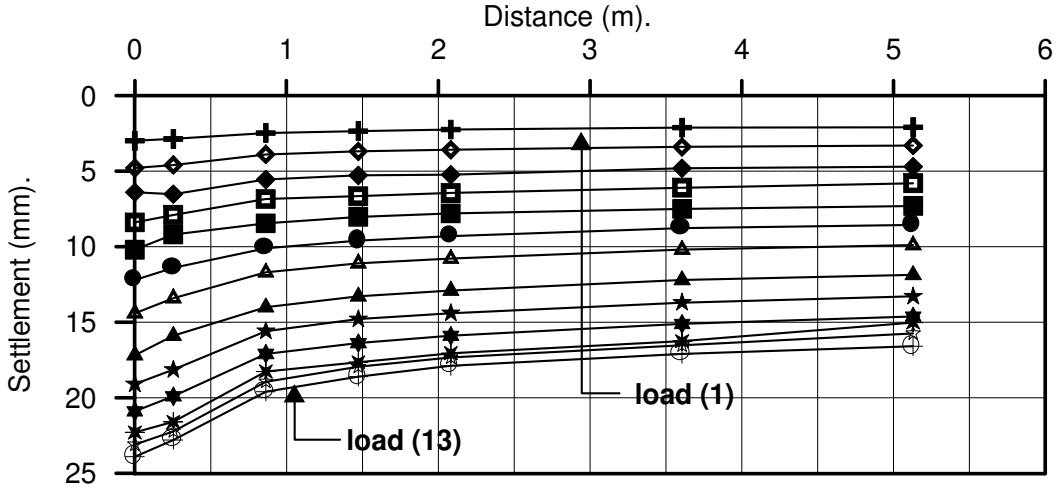

Fig. (3) Surface settlement of the pile and the adjacent soil under different load increments.

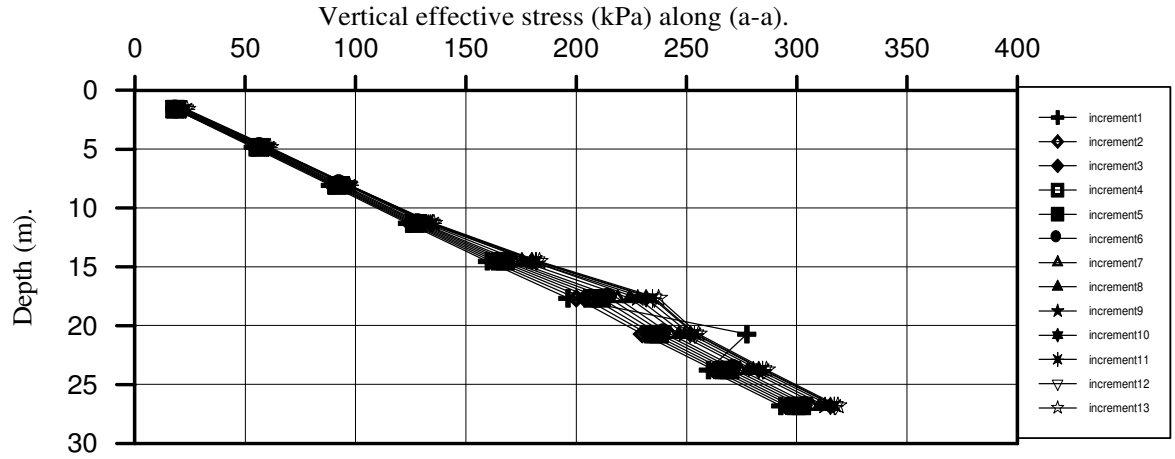

Fig. (4) Vertical effective stress along Sec. (a-a).

Problem No.2

This case represents the loading test, which was done by O'Niell et al. (1982) on (11) closed – ended steel pipe piles in stiff overconsolidated clay. The loading test was mentioned by Castelli and Maugeri (2002). The data was taken from the last reference.

The diameter and penetration depth of the pile used in the analysis was (0.27 m) and (13.10 m), respectively. The total load applied on the pile was (653 kN) through (7) increments. The finite element mesh can be seen in Figure (5).

Material properties:

a. The piles are made of steel, it is assumed to behave as linear elastic (E_s=2.1E8 kPa, υ = 0.15).
b. The behavior of the clay is modelled using the modified Cam-Clay model. Table (3) shows the clay properties that are used in the analysis.

Table (3) Clay properties for the Cam-Clay model of problem No.2.

Type of soil	υ	E_s (kPa)	κ	λ	e_{cs}	M	$\gamma_{(kN/m3)}$	K_o
Clay	0.45	$195*10^3$	0.062	0.161	1.759	0.888	20	0.5

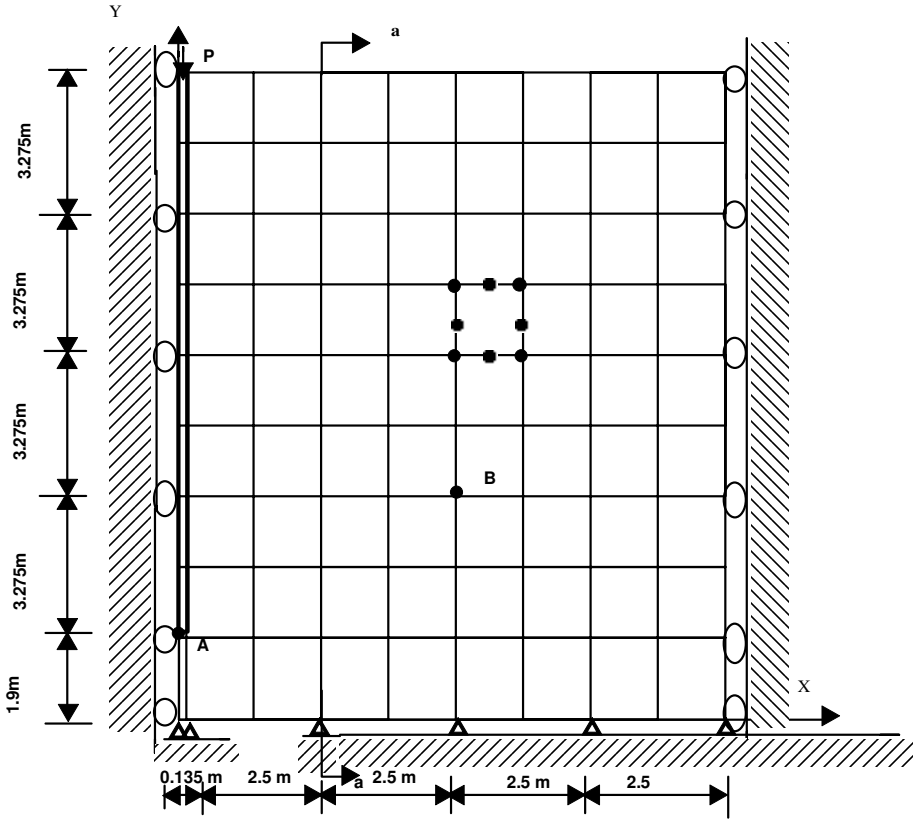

Fig. (5) The finite element mesh for problem No.2.

RESULTS

Figure (6) presents a comparison between the predicated settlements by the finite element method with measured ones. A good agreement between the measured and predicated settlement can be observed. Figure (7) shows the surface settlement that takes place after installation of the pile.

Figure (8) and (9) show the contours of total horizontal stress and total vertical stress, respectively.

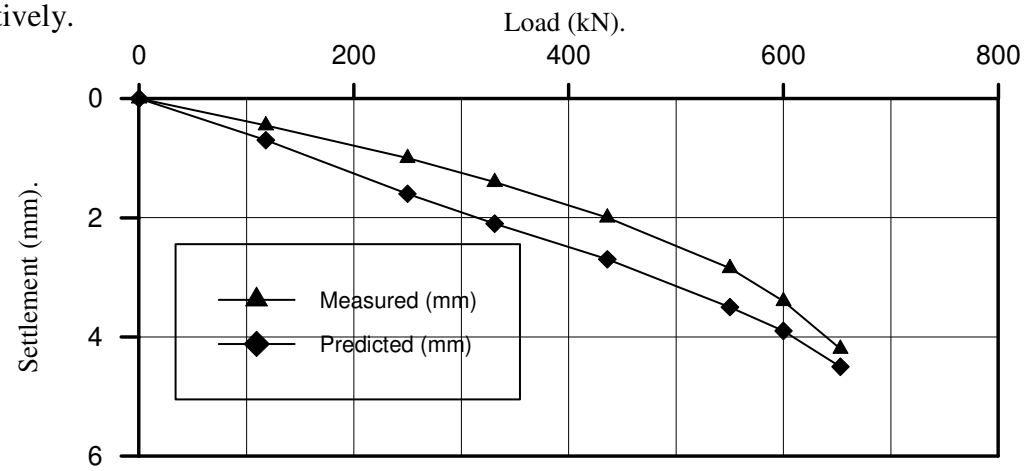

Fig. (6) Load-settlement curve for the pile of problem No.2.

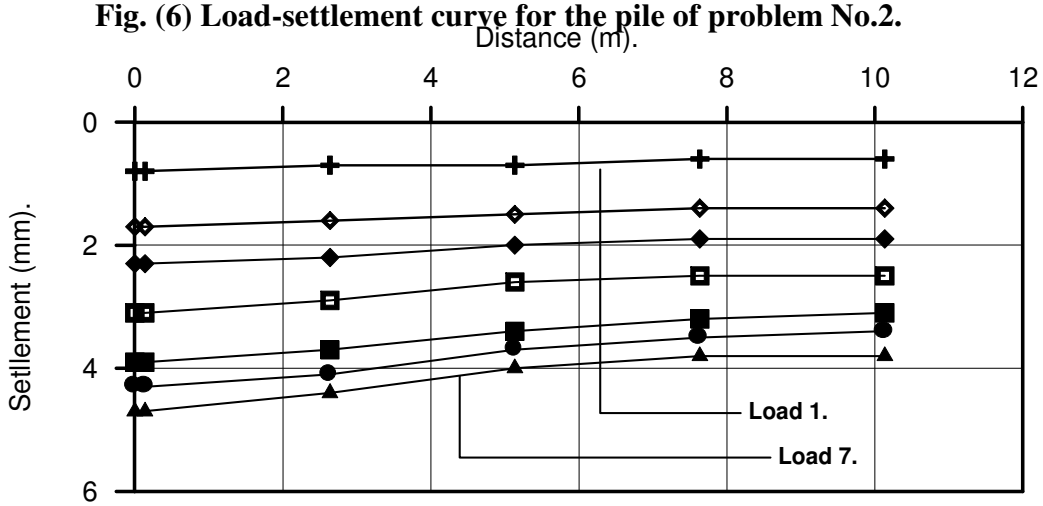

Fig. (7) Surface settlement after pile installation of problem No.2.

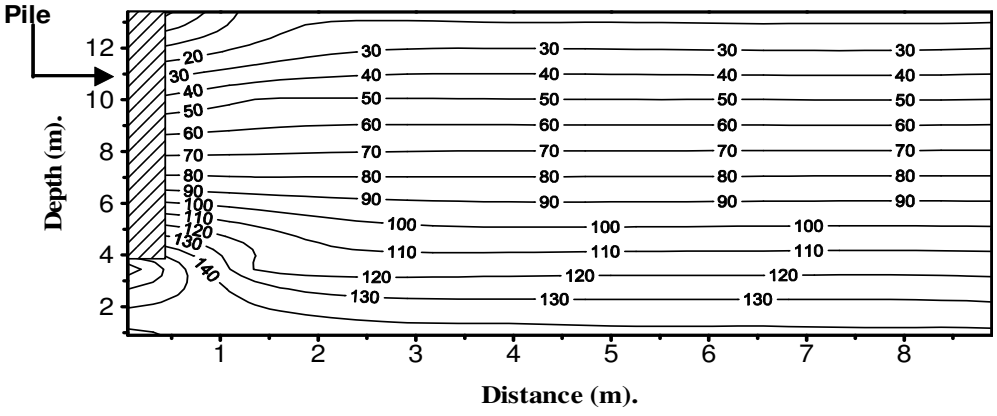

Fig. (8) Contours of total horizontal stress (kPa) of problem No.2.

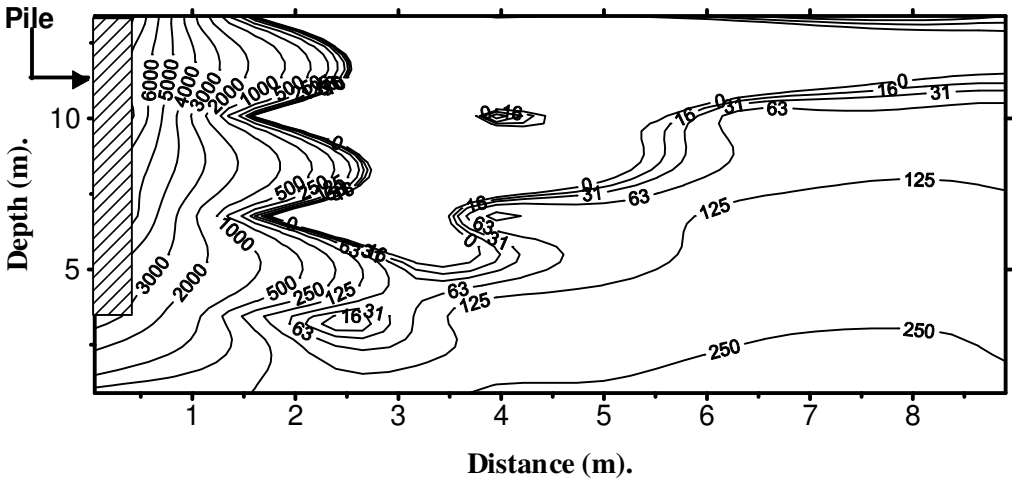

Fig. (9) Contours of total vertical stress (kPa) of problem No.2.

Problem No.3

Pestana et al. (2002) presented full details of field measurements of excess pore pressure and deformation around a 600-mm-diameter, 35-m-long closed –ended steel pile driven into a thick deposit of San Francisco Bay Mud. This study concentrated on the dissipation of generated excess pore pressure due to pile driving through (1000 days) after pile installation.

The project site is located on San Francisco Peninsula in California, near areas of recently completed seismic retrofit work on the I-280 freeway.

Two seismic cone penetration tests with pore pressure measurements were carried out and 8 soil borings were drilled to various depths for the purposes of collecting high-quality laboratory samples and installation field instrumentation at the site.

Piezometer instrumentation

Three piezometer levels were selected at: 8.5, 12.8, and 23.8 m. These depths were chosen to obtain information from both layers of Young Bay Mud and to stay sufficiently far from the sandy drainage layer so that the predominant drainage path would be radial. Nine 1-in-diameter piezometers were installed over a grid representing three depths and three radial distances from the pile where borings 1, 2, and 3 each have two piezometers at nominal depths of 8.5 and 12.8 m, borings 4, 5, 6 have one piezometer each at 23.8 m, boring 7 contains one piezometer at a depth of 6.7 m (Pestana, 2002).

Field monitoring:

The time line of visits to the project site spans a period three years from initial investigations in May 1997 to the final site visit in May 2000. Prior to driving the pile, base line measurement of all instrumentation were obtained. After pile installation, field data were collected frequently in the first days and weeks while the pore pressure gradient was high. These readings became less frequent as the exponential decay of pore pressures continued. The final set of pore pressure measurements was made approximately 2 years after pile installation at which point virtually all pore pressures had dissipated and any changes in the soil were due to secondary effects.

Material properties:

(a) Pile material (steel): Its behavior is considered as linear elastic (E_s=2*10^8 kPa, υ = 0.2).

(b) Soil: the soil profile has been subdivided into five distinct layers:

1) Miscellaneous fill within the upper (3.5m) with $\gamma = 20.4$ kN/m^3.
2) Young Bay Mud between 3.5m-9.75m with $\gamma = 14.3$ kN/m^3.
3) Young Bay Mud between 9.75m-15.5m with $\gamma = 15.1$ kN/m^3.
4) A clayey sand layer from 15.5m-17m with $\gamma = 18.9$ kN/m^3.
5) Young Bay mud below 17m with $\gamma = 16.2$ kN/m^3.

The stiffer sand layer underlying the project site begins at approximately 33.5m. Piezometer measurement gives an approximate ground water table (GWT) at a depth of 2.4m. The k_x k_y properties of these layers can be seen in Table (4).**Table (4) Soil properties for the soils of problem No.3.**

Type of soil	Behavior	E(kN/m^2)	υ	γ(kN/m^3)	κ	λ	M	e_{cs}	k_x (m/s)	k_y (m/s)
Fill	Elastic	2.76E4	0.15	20.4	_	_	_	_	1E-4	1E-4
Young Bay mud(1)	MCC	_	0.45	14.3	0.064	0.324	0.95	2.772	1E-8	1E-8
Young Bay mud(2)	MCC	_	0.45	15.1	0.064	0.324	0.95	2.772	1E-8	1E-8
Clayey sand	Elastic	1.23E4	0.15	18.9	_	_	_	_	1E-4	1E-4
Young Bay mud(3)	MCC	_	0.45	16.2	0.0514	0.257	0.95	2.301	1E-8	1E-8

Note
1) MCC = Modified Cam-Clay.
2) The Modified Cam- Clay properties are calculated according to relations submitted by Randolph, Carter et al.(1978) which are:

$\lambda = 0.00585\ PI$, $\kappa = 0.2\ \lambda$, $e_{cs} = 7\ \lambda + 0.5$.

Table (5) shows the average index properties of San Francisco Bay Mud.

Table (5) Average index properties for San Francisco Bay Mud (after Pestana et al., 2002).

Depth(m)	LL	PL	PI	G_s
8.5	98	39	59	2.75
12.8	86	34	52	2.71
23.8	76	32	44	2.66

RESULTS

Figure (10) presents the finite element mesh. The problem is a coupled one in which the pore pressure is considered as a state variable. The dissipation of excess pore water pressure was studied in several points, and a comparison between field measured (excess pore water pressure) and predicated excess pore water pressure is presented. Both lateral sides are simulated as impervious boundaries.

In this problem a new technique is suggested in which the field measured excess pore water pressures are considered as initial pore pressures in the computer program (CRISP). No load was applied on the pile.

Figure (11) shows a comparison between the measured and predicted pore water pressure (PWP) at a point (0.55, 8.5) m from the pile face, while Figure (12) shows the comparison at a point (0.55, 12.8) m from the pile face. Figure (13) presents the comparison at a point (1.07, 23.8) m from pile face. A good agreement between the field and predicated excess pore water pressures can be seen in all cases.

Also a comparison between the actual and predicated (degree of consolidation) at the same points is introduced. The degree of consolidation U is calculated according to the following equation:

$$U(\%) = \frac{(u_i - u)}{(u_i - u_o)} \qquad \text{.....(1)}$$

where :

u_i is the initial excess pore water presure.

u is the excess pore water pressure at any time.

u_o is the hydrostatic pore water pressure.

Figure (14) shows the comparison at a point (0.55, 8.5) m from the pile face. In this figure, the predicated degrees of consolidation are close to the measured values and show good agreement.

Measuring lateral deformations would provide information on the consolidation process as the generated excess pore pressure dissipated, so the distribution of horizontal displacement along the pile at section (a-a) (shown in Figure (10)) is presented in Figure (15). It can be noticed that at different locations, there are sudden increases in lateral displacement due to presence of layers of different properties, in addition to the presence of interface element at the base of the pile which permits smooth movements to take place for the soil at the pile base.

The change in vertical effective stress along section (a-a) with time is presented in Figure (16). The changes in horizontal effective stress and pore water pressure along section (a-a) with time are presented in Figures (17) and (18), respectively.

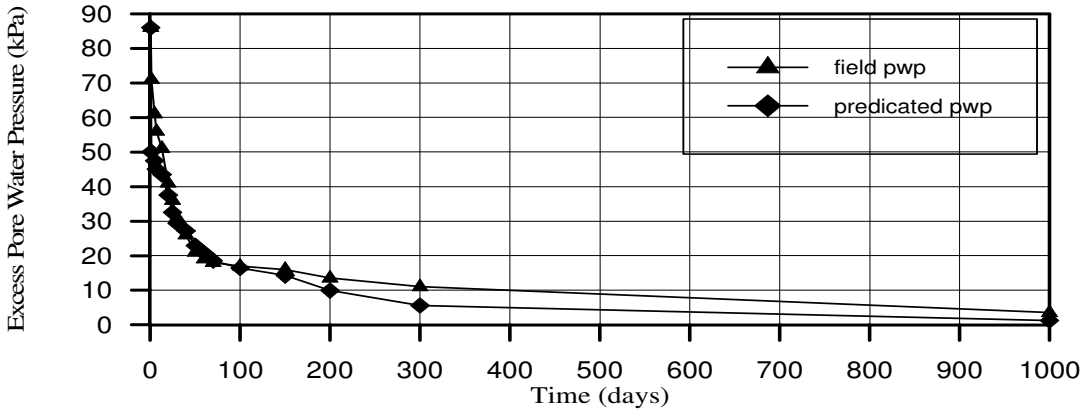

Fig. (10) The finite element mesh of the problem No.3.

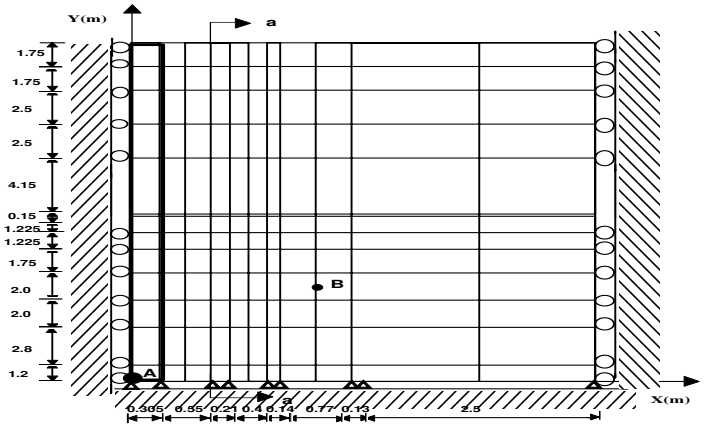

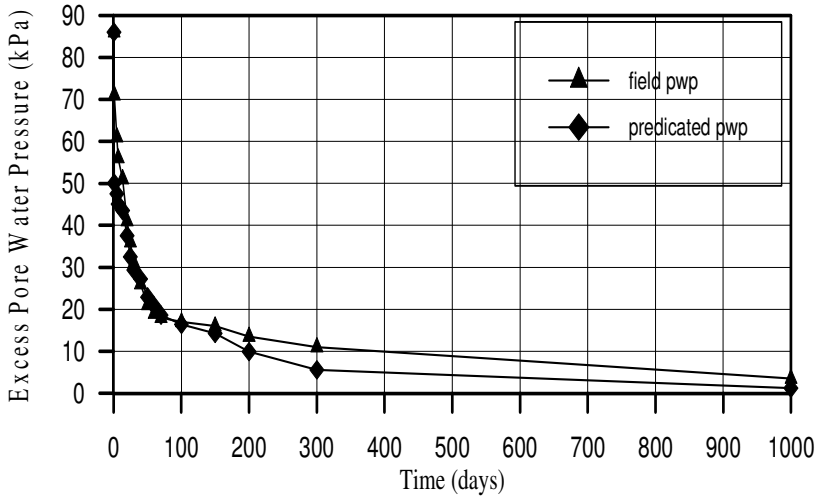

Fig.(1.12) Dissipation of excess pore water with time at a point located at a distance 0.55 m from the pile face and depth 8.5 m.

(11) Dissipation of excess pore water pressure with time at a point located at a distance 0.55 m from the pile face and depth 8.5 m.

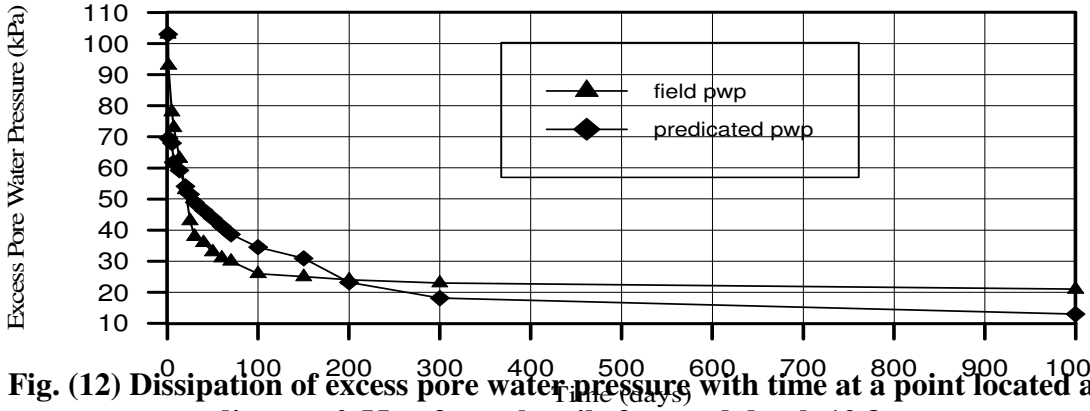

Fig. (12) Dissipation of excess pore water pressure with time at a point located at a distance 0.55 m from the pile face and depth 12.8 m.

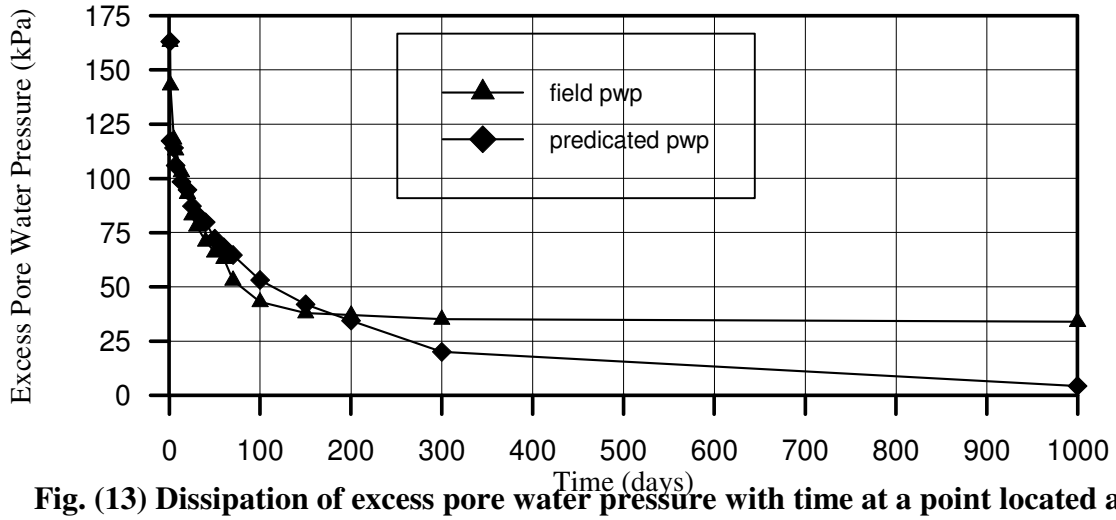

Fig. (13) Dissipation of excess pore water pressure with time at a point located at a distance 1.07 m from the pile face and depth 23.8 m.

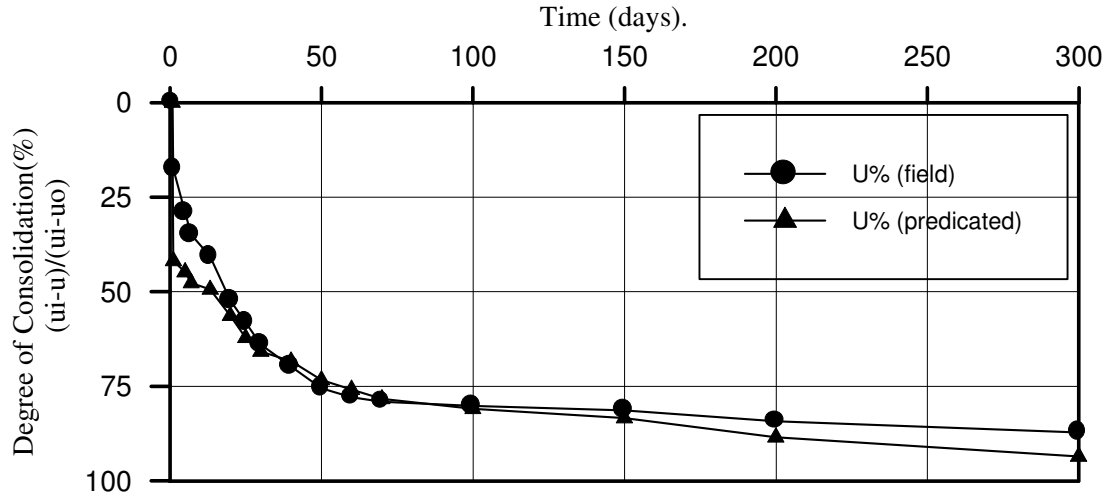

Fig. (14) Variation of degree of consolidation with time at a point (0.55 m) from the pile face and at a depth (8.5 m).

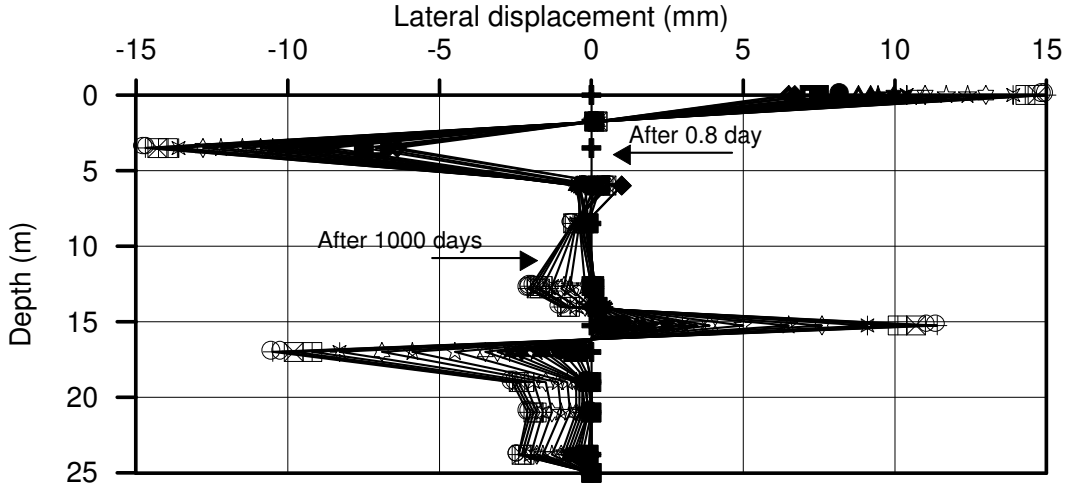

Fig. (15) Lateral displacement along Sec. (a-a) of the problem No.3.

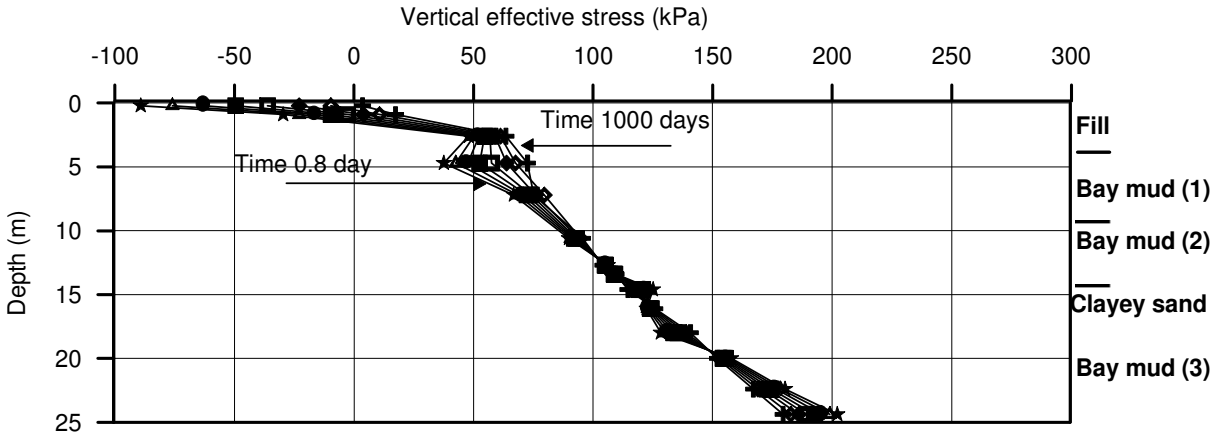

Fig. (16) Changes in vertical effective stresses along Sec. (a-a) of problem No.3.

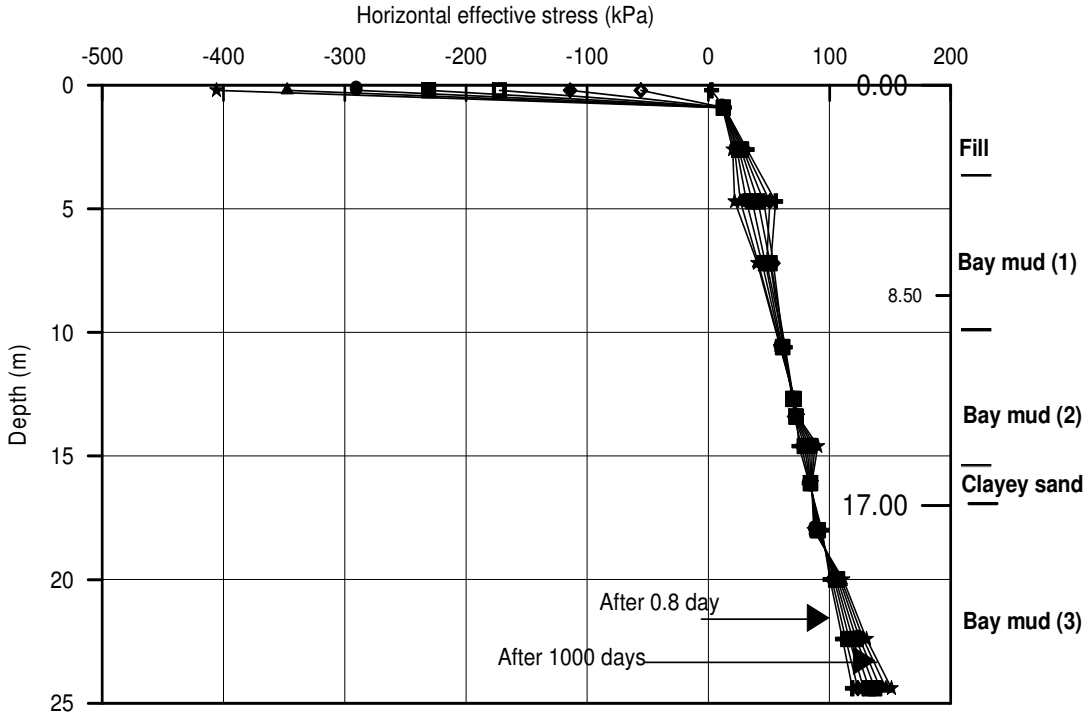

Fig. (17) Changes in horizontal effective stresses along Sec. (a-a) of problem No.3.

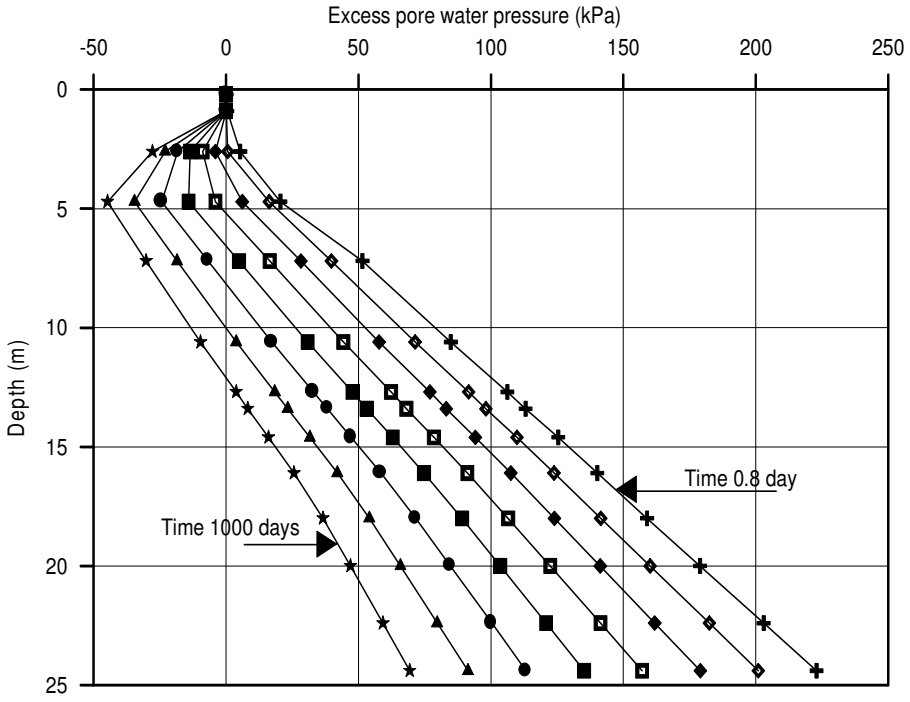

Fig. (18) Change in pore water pressure along Sec. (a-a) of problem No.3.

Conclusions

The finite element analysis of some pile- soil interaction problems revealed the following conclusions:

1. Good agreement between the measured and predicted settlements by the finite element method when the soil is assumed to follow the modified Cam Clay model.
2. The proposed technique used in this paper, in which the measured excess pore water pressures are considered as initial pore pressures in the computer program (CRISP). No load was applied on the pile. The dissipation of excess pore water was studied through carrying out consolidation analysis.
3. The analysis of pile embedded in layered soil showed that the distribution of horizontal displacement in the soil adjacent to the pile indicates sudden increases in lateral displacement. This may be attributed to the sudden change in the properties of the different layers in addition to the presence of the interface element at the base of the pile which permits smooth movements to take place for the soil at the pile base.

References

- Al-Assady A. K. M., (1998); "Effect of anisotropy on two-dimensional consolidation of clayey soil", a Thesis submitted to Civil Eng. Dept. in the University of Baghdad for degree of Master.
- Al-Chalabi J. H.H., (1990); "Single pile analysis using finite element method", a Thesis submitted to Civil Eng. Dept. in the University of Basra for the degree of Master.

- Britto A. M. and Gunn M. J., (1987); "Critical state soil mechanics via finite elements", John Wiley and Sons, New York, U.S.A.
- Castelli F. and Maugeri M., (2002); "Simplified nonlinear analysis for settlement prediction of pile groups", Journal of Geotechnical and Geoenvironmental Engineering, January, ASCE, vol.128, No.1, P.P. 76-83.
- Desai C. S., (1974); "Numerical design-analysis for piles in sands", Journal of the Geotechnical Engineering Division, vol.100, No.6, P.P. 613-635.
- Grande L. and Nordal S., (1979); "Pile-soil interaction analysis on effective stress basis", Recent Developments in the Design and Construction of Piles, ICE, London.
- Hunt C. E., Pestana J. M., Bray J. D. and Riemer M., (2002); " Effect of pile driving on static and dynamic properties of soft clay", Journal of Geotechnical and Geoenvironmetal Engineering, January, ASCE, vol.128, No.1, P.P. 13-23.
- Kirby R.C. and Esrig M.I., (1979); "Further development of a general effective stress method for prediction of axial capacity for driven piles in clay", Recent Developments in the Design and Construction of Piles, ICE, London.
- Pestana J. M., Hunt C. E. and Bray J. D., (2002); "Soil deformation and excess pore pressure field around a closed-ended pile", Journal of Geotechnical and Geoenvironmental Engineering, January, ASCE, vol.128, No.1, P.P. 1-12.
- Randolph M. F. and Wroth C. P., (1978); "Analysis of deformation of vertically loaded piles", Geotechnique, Vol. 104, No.12, P.P. 1465-1488.
- Randolph M. F. and Wroth C. P., (1981); "Application of the failure state in undrained simple shear to the shaft capacity of driven piles", Geotechnique 31, No.1, P.P. 143-157.